PERFORMANCE INVESTIGATION OF INNOVATIVE COMPACT POROUS CERAMIC HEAT EXCHANGER

Abstract :

It is critical to design efficient and compact heat exchangers in order to improve the energy use rate, thus increasing the overall energy system efficiency. In this study, the performance of an innovative configuration of a compact porous ceramic heat exchanger has been investigated. A numerical model capable of assessing heat and mass transport within an unsaturated porous ceramic exchanger has been carefully built based on Whitaker theory. To model the transport processes that occur during convective exchange, a three-dimensional unstructured Control Volume Finite Element Method (CVFEM) is developed. Several numerical tests have been carried out in this regard. The effect of porosity, hot air velocity and ceramic initial saturation have been investigated. The temperature, liquid saturation, and pressure evolutions of the porous domain are studied and compared over time. It is observed from the results that the porosity of ceramic material is vital to maximize the heat exchange. The use of ceramic has 0.1 porosity results in time savings of 55% compared to the reference case corresponding to 0.7 porosity. Furthermore, the findings demonstrate that increasing the air velocity by a factor of two reduces the exchanging time by half when compared to the reference case corresponding to hot air velocity V=5m/s.

Keywords: *heat and mass transfer, ceramic heat exchanger, CVFEM, porous media*

1. Introduction

Heat transmission has recently been the subject of numerous studies. Heat transfer is found in many conversion systems and devices that involve the use of heat exchangers. As a result, porous media, which significantly improve heat and mass transport, have seen a variety of industrial applications. It's worth noting that more study on porous media's potential, especially on heat exchangers, is necessary. In this study, the focus will be on examining heat and mass transfer within unsaturated porous ceramic exchangers.

The development of a numerical model was presented and described. This model predicts heat and mass transport based on the Whitaker theory, it uses a three-dimensional unstructured Control Volume Finite Element Method to evaluate the convective exchange process with various operating parameters, aiming at a parametric study for achieving optimal thermal performance and overall efficiency for the compact heat exchanger under consideration [**1**]. Intrinsic permeability and inertial coefficients are taken into account, respectively determined by empirical correlations related to the

porous core's geometric characteristics [**2**]. According to the numerical experiments, heat transfer rates and the average outlet fluid temperature were improved when porosity was decreased for several mass flow rates [**3**]. Optimization potential can be achieved in terms of pore morphology and materials, and structure design for new more mechanically robust and longer lasting structure [**4**].

Characterization of the porous structure is important to understand the implications of any changes that are made to their performance and to help in an efficient design. In fact, the minimization of thermal resistances, during the design of compact heat exchangers, leads to an improvement of heat transfer and a reduction of thermal dissipation [**5**]. An open-cell foams' multiscale model was established and studied to cover different materials, cell sizes, and porosities for a proper characterization of the heat exchanger [**6**]. In the model, it was possible to obtain a complete description of the porous material by a set of main properties of porous media, such as pressure loss coefficients, heat conductivity, and Nusselt numbers in porous media, especially in anisotropic media [**7**]. This data can be used as input for a macroscopic model in order to predict the global performance of the entire device.

The important detail is that, in this case, it is not the Rosseland type of modeling (simple) but a multilayered model that characterizes the microstructure of porous ceramic foam and that can be an input for macroscopic modeling. In fact, the flow motion's complex effect on the heat transfer process occurring in porous media, over a spatial problem in the porous domain, requires a robust numerical method and an efficient meshing that can characterize the fluid-solid interface interface [**8**]. The porous medium's morphological characteristics (aspect of the pores like pore size distribution, connectivity) also have an impact on the effective thermal conductivity and the permeability and they directly affect the thermal-hydraulic performance of the exchanger [**9**].

The potential of materials with a high specific surface area has been tested for the design of high-performance heat transfer applications including compact heat exchangers [**10**]. The porous structure's geometry has a direct impact on thermal and fluid dynamic responses, and a multiscale modeling approach can be introduced to optimize the advanced ceramic heat exchanger design [**11-12**].

Thermal conductivity as a design input parameter for a heat transfer device can affect its overall performance [**13**]. Macroscopic models with effective transport properties can be derived by direct pore-level numerical simulations of complex porous geometry [**14-15**]. Optimization of the design of the heat exchanger is needed because porous materials' complex anisotropic nature is a challenging task [**16-14**].

In conclusion, this study is aiming at an investigation of the coupled heat and mass transfer in a porous compact ceramic exchanger using a 3-D numerical model. The model was based on Whitaker theory using the Control Volume Finite Method. The influence of porosity, hot air velocity, and initial ceramic saturation has been studied by variations of temperature, liquid saturation, and pressure during the considered time in the porous domain.

2. Problem statement and Formulation

The present problem is a numerical study of heat and mass transfer inside a porous ceramic heat exchanger. The schematic diagram of porous compact heat exchanger is shown in Fig. 1. The material of the Heat exchanger is of ceramic with the width, length and height of 8 cm, 10 cm and 8cm, respectively. The ceramic domain is supposed to be unsaturated porous material with porosity 0.7, 0.5, 0.3 and 0.1 respectively are considered in the current study.

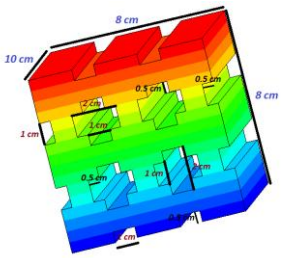

Fig. 1. Porous heat exchanger geometry.

2.1. Numerical equations

The system of equations is defined by a reference to Whitaker's theory [**17**]. A numerical model of heat and mass transfer is established for the unsaturated porous media and the following assumptions have place:

- We consider that the porous medium is homogenous and isotropic and the three phases (solid, liquid, gas) are in local thermodynamic equilibrium.
- We neglect the viscous dissipation, the compression-work and the radiative heat transfer.
- The gaseous phase is ideal (thermodynamic sense) and the dispersion and tortuosity terms are used as diffusion term.

In this context, the macroscopic equations of heat and mass transfer in porous media are:

- **Generalized Darcy's Law:**

Referring to Darcy's law, the average velocities (liquid phase ($\overline{V_l}$) and gaseous phase ($\overline{V_g}$)) are defined as bellow (Eq. (1)):

- ***Liquid:***

$$\overline{V_l} = -\frac{KK_l}{\mu_l}\left[\nabla\left(\overline{P_g}^{g} - P_c\right) - \overline{\rho_l}^{l} g\right] \quad (1)$$

And $P_c = \overline{P_g}^g - \overline{P_l}^l$ presents the capillary pressure.

- ***Gas (without applying the gravitational effect) (Eq. (2)):***

$$\overline{V_g} = -\frac{KK_g}{\mu_g}\nabla\overline{P_g}^g \tag{2}$$

- **Mass conservation:**

- ***Liquid:***

The equation of mass conservation for liquid phase is (liquid density is constant) (Eq. (3)):

$$\frac{\partial \varepsilon_l}{\partial t} + \nabla(\overline{V_l}) = -\frac{\dot{m}}{\overline{\rho}_l} \tag{3}$$

With $\dot{m}$: the rate mass of the evaporation and ε_l : the fraction volume of liquid

- ***Gas:***

The equation of mass conservation for gaseous phase is (Eq. (4)):

$$\frac{d\overline{\rho_g}}{dt} + \nabla\left(\overline{\rho_g}^g \overline{V_g}\right) = \dot{m}_g \tag{4}$$

With $\overline{\rho}_g^g$: the average density intrinsic of gaseous phase.

- ***Vapor (Eq. (5) and (6)):***

$$\frac{d\overline{\rho_v}}{dt} + \nabla\left(\overline{\rho_v}^g \overline{V_v}\right) = \dot{m}_v \tag{5}$$

$$\overline{\rho}_v^g \overline{V}_v = \overline{\rho}_v^g \overline{V}_g - \overline{\rho}_g^g D_{eff} \nabla\left(\frac{\overline{\rho_v}}{\overline{\rho_g}^g}\right) \tag{6}$$

D_{eff} presents the effective diffusion coefficient of vapor in porous medium.

- **Energy conservation:**

The equation of energy conservation is defined as bellow (Eq. (7)):

$$\frac{\partial}{\partial t}(\overline{\rho C_P}\overline{T}) + div\left[\left(\overline{\rho_l}^l C_{Pl}\overline{V_l} + \sum_{k=a,V}\overline{\rho_k}^g C_{Pk}\overline{V_k}\right)\overline{T}\right] = \nabla\left(\lambda_{eff}.\nabla\overline{T}\right) - \Delta H_{vap}\ \dot{m}_v \tag{7}$$

With ΔH_{vap} : heat latent of vaporization at temperature T(K).

λ_{eff} : thermal effective conductivity of porous medium.

$\overline{\rho C_p}$: heat capacity of the porous medium defined as bellow (Eq. (8)):

$$\overline{\rho C_p} = \bar{\rho}_s C_{ps} + \bar{\rho}_l C_{pl} + \bar{\rho}_a C_{pa} + \bar{\rho}_v C_{pv} \quad (8)$$

Which $\bar{\rho}_s C_{ps}$, $\bar{\rho}_l C_{pl}$, $\bar{\rho}_v C_{pv}$ and $\bar{\rho}_a C_{pa}$ presents the mass heat capacities of three phases (solid, liquid, vapor and air).

- **Thermodynamic relations:**

The partial pressure of vapor is defined as bellow:

$P_v = P_{veq}(T, S)$.

With S: saturation of liquid explained by (Eq. (9)):

$$S = \frac{\varepsilon_l}{\varepsilon} \quad (9)$$

For the gaseous phase, the pressure is (Eq. (10)):

$$\bar{P}_i = \frac{\bar{\rho}_i}{M_i} R \bar{T} \;; i=a,v \quad (10)$$

$$\bar{P}g = \bar{P}a + \bar{P}v \,,\; \bar{\rho}g = \bar{\rho}a + \bar{\rho}v$$

For the vapor, the pressure is defined by (Eq. (11)):

$$\frac{Pv}{Pvs} = \exp\left(-\frac{2.\sigma.M_v}{r.\rho_l.R.T}\right) \quad (11)$$

2.2. Boundary and initial conditions

Initially, all fields; the temperature, saturation and pressure are uniform in the heat exchanger domain (Fig. 2).

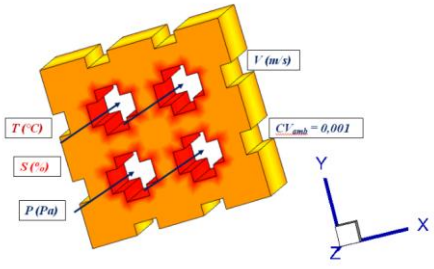

Fig. 2. Exchanger's boundary conditions.

The boundary conditions for our model are defined as following:

The exchanging cavities (highlighted in red in Fig.1) (Eq. (12)):

$$\left[\lambda_{eff}\frac{\partial\langle T\rangle}{\partial X_i}+\Delta H_{vap}\rho_l\langle V_l\rangle n_i\right]=h_t\left(\langle T\rangle-T_\infty\right) \tag{12}$$

The mass flow (evacuation and evaporation) (Eq. (13)):

$$\left[\rho_l\langle V_l\rangle+\langle\rho_v\rangle^g\langle V_v\rangle\right]n_i=h_m\left(C_{vs}-C_{v\infty}\right) \tag{13}$$

On exchanging cavities, the pressure is considered as the atmospheric pressure (Eq. (14)):

$$\left[\langle P_g\rangle^g\right]=P_{atm} \tag{14}$$

The external faces (right, left, up, bottom) are considered as adiabatic and impermeable faces.

$$\left[\lambda_{eff}\frac{\partial\langle T\rangle}{\partial X_i}+\Delta H_{vap}\rho_l\langle V_l\rangle n_i\right]=0 \tag{15}$$

$$\left[\rho_l\langle V_l\rangle+\langle\rho_v\rangle^g\langle V_v\rangle\right]n_i=0 \tag{16}$$

$$\left[\frac{\partial\langle P_g\rangle^g}{\partial X_i}\right]=0 \tag{17}$$

The convective coefficients (heat and mass transfer) are presented in Table. 1.

Table. 1. Convective coefficients for heat and mass transfer.

	Cavities [18]	**Faces [19]**
h_t	$\frac{\lambda\times 0.023\times \mathrm{Re}^{4/5}\times \mathrm{Pr}^{1/3}}{D}$	$\frac{\lambda\times 0.023\times \mathrm{Re}^{4/5}\times \mathrm{Pr}^{1/3}}{L_C}$
h_m	$\frac{D_{A,B}\times 0.023\times \mathrm{Re}^{4/5}\times \mathrm{Sc}^{1/3}}{D}$	$\frac{D_{A,B}\times 0.023\times \mathrm{Re}^{4/5}\times \mathrm{Sc}^{1/3}}{L_C}$
Validity	$10^4 < Re < 1.2\times 10^5$ $0.6 \le \mathrm{Pr} \le 160$ $0.6 \le \mathrm{Sc} \le 160$	$\mathrm{Re} < 5\times 10^5$ $\mathrm{Pr} \ge 0.6$ $\mathrm{Sc} \ge 0.6$
Re	$\frac{\rho_a w_a D}{\mu_a}$	$\frac{\rho_a w_a L_C}{\mu_a}$

$$\mathrm{Pr} = \frac{C_a \mu_a}{\lambda_a} \qquad \mathrm{Sc} = \frac{\vartheta_a}{D_{A,B}}$$

Which:

h_t : Convective coefficient of heat transfer [Wm-2°C-1]

h_m: Convective coefficient of mass transfer [ms-1]

$D_{A,B}$: Vapor diffusion in air defined as bellow:

$D_{A,B} = D_{vap,air} = 0.26 \times 10^{-4}\ [m2s-1]$

$L_C = 0.1$ m presents the characteristic length of the exchanger.

3. Numerical solution, grid dependency and validation

The Control Volume Finite Element Method (CVFEM) is used to solve our system of equations [**20-21**]. Moreover, the control volume is composed of prismatic elements which ensures the grid flexibility and the conservation of flux.

For the mesh generation, the free mesh generator Gmsh is employed (Fig. 3). The heat exchanger domain is divided in six-node prisms. Also, the centroids of the triangular elements (prism's base) are joined to the midpoints of the corresponding sides.

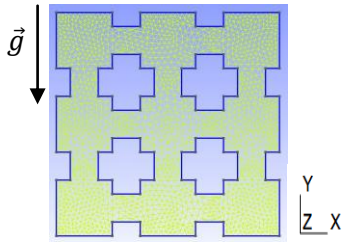

Fig. 3. Cross section of the 3D domain meshing.

- **Grid dependency**

Because of the relevance of grid size on the accuracy of numerical findings, grid independency tests were carefully performed. The initial and operating conditions are depicted in Table. 2.

Table. 2. Initial and operating conditions for the validation tests.

Initial temperature	Initial saturation	Hot air temperature	Hot air velocity	porosity
20°C	50%	100°C	20m/s	0.1

- **Model validation**

A numerical code (Fortran) has been developed to solve the coupled heat and mass transfer equations. The model is validated by the study of Hussain et al. [**22**]. With the great agreement shown in Fig. 4, it can be concluded that the model developed to simulate mass and heat transport within porous exchangers is accurate and reliable enough to be used in this investigation.

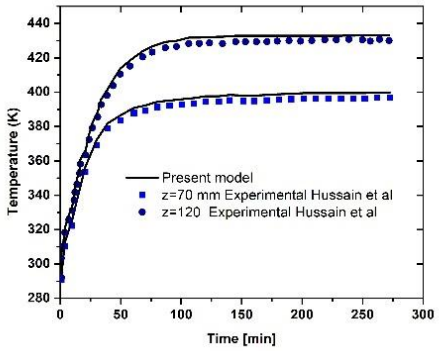

Fig. 4. Evaluation of the current model's transient temperature results compared to those of Hussain et al. [22], at two different axial locations.

4. Results and discussions

In this section, we present the numerical results obtained for the simulation of heat and mass transfer within the considered compact porous exchanger.

The findings section is composed of three parts: Effect of hot exchanging air temperature ; Effect of initial saturation of porous domain ; Effect of porosity ; Effect of hot air velocity.

4.1. Effect of hot exchanging air temperature

In this part, the effect of the hot exchanging air temperature has been evaluated. Therefore, four cases have been tested (Table. 3).

Table. 3. Operating and initial conditions for four studied cases.

	T (°C)	**S_{in}** (%)	**T_{in}** (°C)	**V** (**m/s**)	**PO** -	**CV_{amb}**	**P_{amb}** (**atm**)
Case A	100	50	20	5	0.1	0.001	1
Case B	80	50	20	5	0.1	0.001	1
Case C	60	50	20	5	0.1	0.001	1

Case D	40	50	20	5	0.1	0.001	1

Fig. 5 shows that the time evolution of the averaged porous domain temperature is highly affected by the hot air temperature and the initial saturation. Fig. 6 demonstrates that the fastest exchange corresponds to the lowest initial liquid saturation. Moreover, the gaseous pressure inside the porous ceramic (Fig. 7) shows that the highest-pressure peak corresponds to case A where highest air temperature and initial saturation are used.

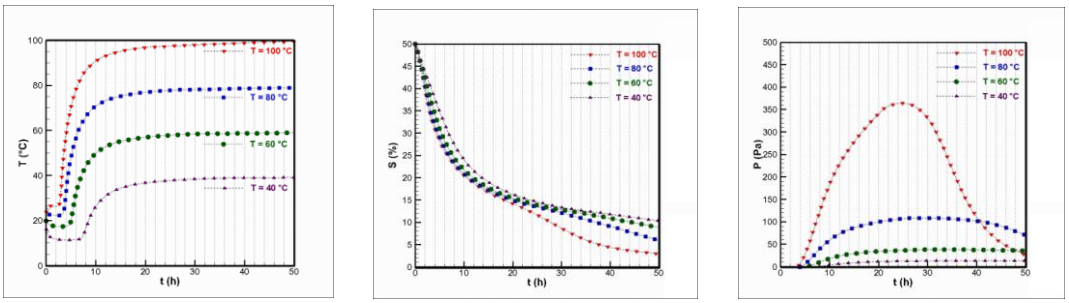

Fig. 5. Time evolution of temperature. Fig. 6. Time evolution of saturation. Fig. 7. Time evolution of pressure.

4.2. Effect of initial saturation of porous medium

In this part, the effect of the initial saturation of porous medium has been evaluated. Therefore, four cases have been tested (Table. 4).

Table. 4. Operating and initial conditions for four studied cases.

	T (°C)	**S_{in}** (%)	**T_{in}** (°C)	**V** (**m/s**)	**PO** -	**CV_{amb}**	**P_{amb}** (**atm**)
Case A	100	50	20	5	0.1	0.001	1
Case B	100	40	20	5	0.1	0.001	1
Case C	100	30	20	5	0.1	0.001	1
Case D	100	20	20	5	0.1	0.001	1

Fig. 8 shows that the time evolution of the averaged porous domain temperature is highly affected by the initial saturation. Since the ceramic is considered as unsaturated porous medium where the mixture air and water coexist in the pores. Fig. 9 demonstrates that the fastest exchange

corresponds to the lowest initial liquid saturation. The gaseous pressure inside the porous ceramic (Fig.10) shows that the highest-pressure peak corresponds to case A where highest air temperature and initial saturation are used.

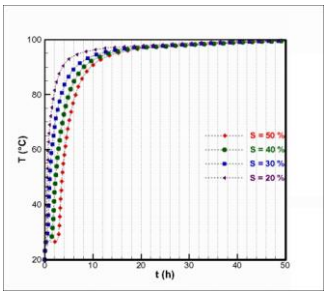

Fig. 8. Evolution of temperature.

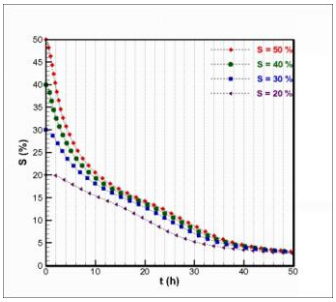

Fig. 9. Evolution of Saturation.

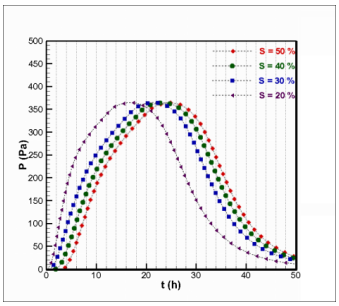

Fig. 10. Evolution of pressure.

4.3. Effect of porosity

Referring to Fig. 11, representing the 3D distributions of temperature, saturation and pressure inside the porous medium at 3h, since only the cavities are exchanging mass and heat within the hot circulating air, it can be seen that the heat propagates through the exchanging cavities to the whole porous ceramic domain. The decrease in porosity leads to higher heat exchange and faster thermal diffusion occurs in the vicinity of the exchanging cavities at earlier stages compared to higher porosities. The high porosity favorizes the migration of liquid towards the exchange cavities but since the larger porosities results in larger water quantities so larger amount of heat are consumed to evaporate water before increasing the overall ceramic temperature and reaching the thermal equilibrium. This implies a faster exchange time is obtained for low porosity. Moreover, the increase of porosity implies the presence of larger water quantity inside the exchanger, which results in a higher-pressure profile.

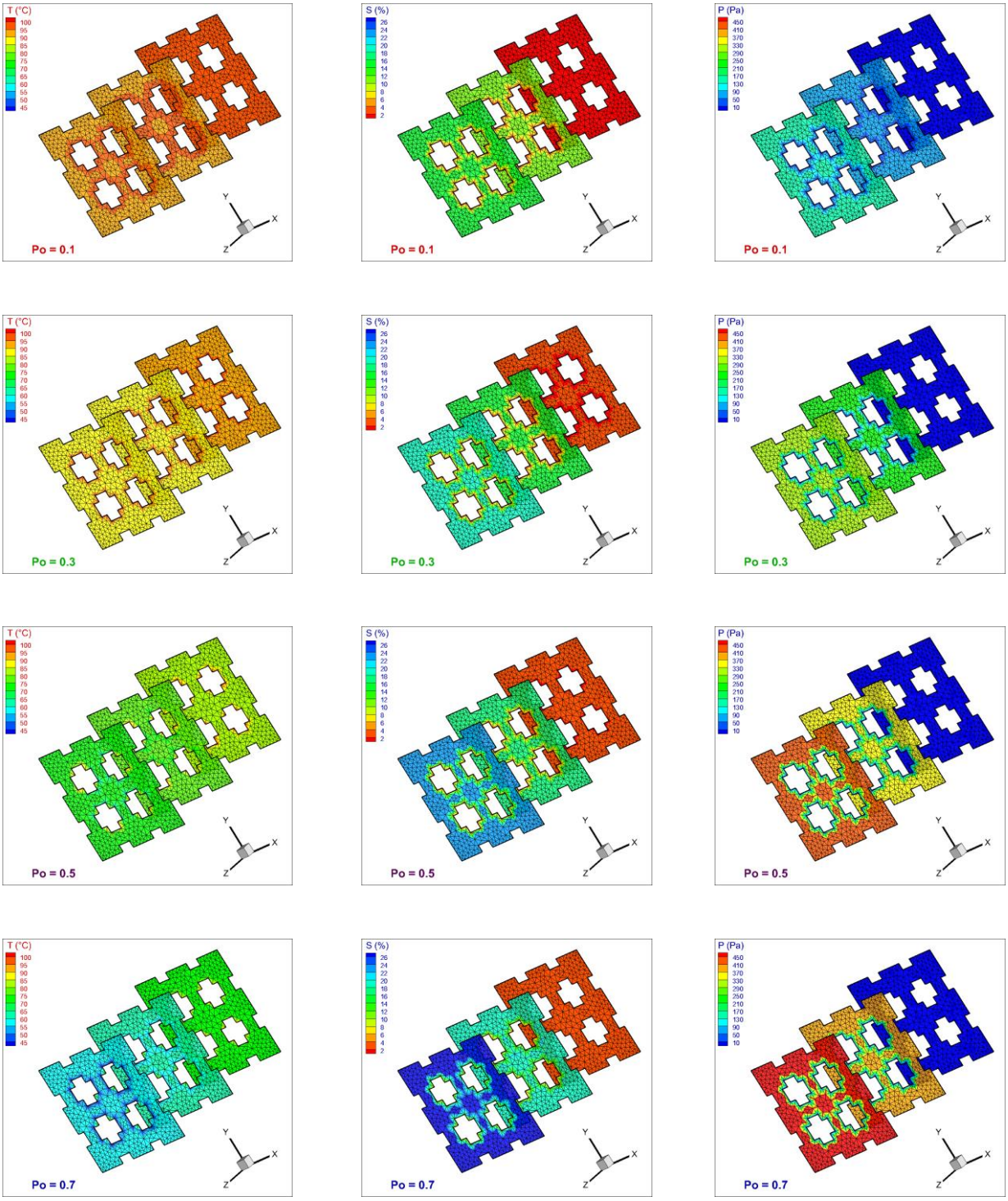

Fig. 11. 3D distributions of temperature, saturation and pressure for different porosity values after 3h.

4.4. Effect of hot air velocity

The slices' view to represent the distribution of temperature, liquid saturation, and gaseous pressure for different velocity values after 3h are depicted in Fig. 12. The increase of the velocity induces an intense and rapid heat exchange detected by high temperature near the exchanging cavities. Likewise, lower liquid saturation is noticed near the exchanging cavities at early stage for high air velocities. As a result, for high velocity, high pressure is seen inside the ceramic which is responsible for water extraction to the exchanging surfaces. Such behaviour can be explained by strengthening of the heat and mass transfer coefficients that lead to intense exchange and high temperature field within the porous ceramic HX.

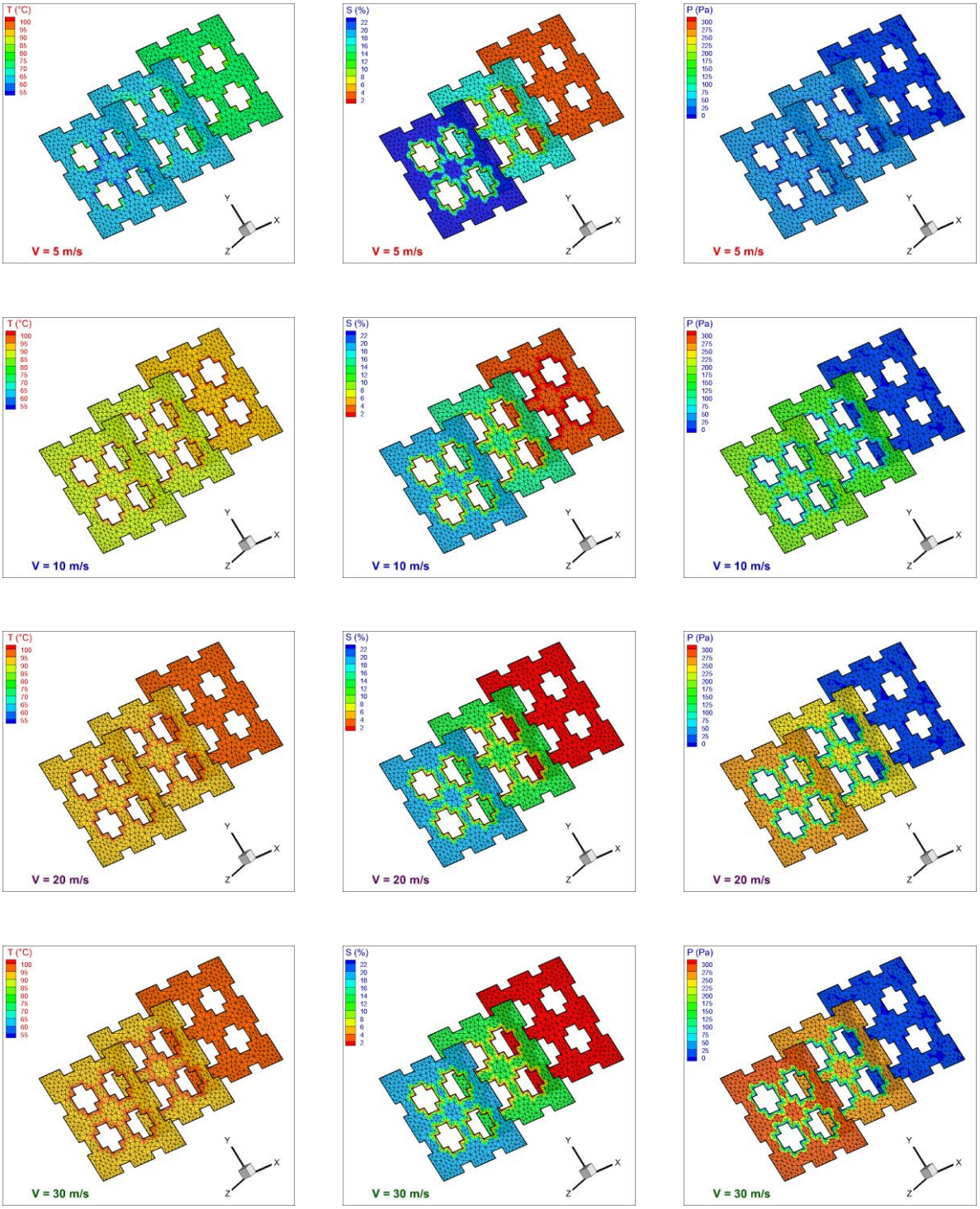

Fig. 12. 3D distributions of temperature, saturation and pressure for different air velocities after 3h

5. Conclusions

In the present study, a 3-D numerical model is established to analyze the effects of parameters (temperature, saturation, porosity and hot air velocity) on heat and mass transfer within a porous compact heat exchanger. The mesh was generated by the free mesh generator Gmsh and a Fortran numerical code has been developed. The numerical model successfully describes the effect of the temperature, liquid saturation, porosity, and hot air velocity on the thermal exchanging rate. From the computation results following conclusions are drawn:

- The operating conditions related to initial saturation and hot air temperature should be carefully chosen. Heat exchange rate increases with decrease in initial liquid saturation of the porous ceramic medium.
- Heat transfer coefficient increases with increase of hot air velocity leading to intense and rapid heat exchange. Likewise, the mass transfer efficiency increases with air velocity increase.
- The porosity of ceramic material is vital to maximize the heat exchange; the use of ceramic has 0.1 porosity results in time savings of 55% compared to the reference case corresponding to 0.7 porosity.
- The case corresponding to air velocity V=30m/s, leads to a time saving of 81% comparing to the case where V=5m/s.
- The findings demonstrate that increasing the air velocity by a factor of two reduces the exchanging time by half when compared to the reference case corresponding to hot air velocity V=5m/s.

DATA AVAILABILITY STATEMENT

All data generated or analyzed during this study are included in this published article.

Nomenclature

C_a	specific heat of the air $[kJkg-1k-1]$	Greek letters	
C_p	specific heat at constant pressure $[kJkg-1k-1]$	ε	porosity
C_v	specific heat of the vapor $[kJkg-1k-1]$	ε_l	volume fraction of liquid phase
C_w	specific heat of the water $[kJkg-1k-1]$	μ	dynamic viscosity [kg m-1 s-1]
$D_{A,B}$	Diffusion coefficient [m2s-1]	ϑ	kinematic viscosity $[m2\ s-1]$
g	gravitational acceleration [m s-2]	ρ	density [kg m-3]
h_m	convective mass transfer coefficient$[ms-1]$	λ	conductive transfer coefficient $[Wm-1°C-1]$
h_t	convective heat transfer coefficient$[Wm-2°C-1]$	σ	surface tension $[N\ m-1]$
K	intrinsic permeability [m2]	ΔH_{vap}	vaporisation latent heat [J kg-1]
L_c	characteristic length of brick [m]		
M	molar mass of air [kg mol-1]	Subscripts	
		0	initial condition
ṁ	evaporation rate [kg s-1]	a	air
n_i	outward normal vector	eff	effective
P	pressure [Pa]	g	Gas
Pc	capillary pressure [Pa]	l	liquid
Po	Exchanger porosity [%]	v	vapor
P_{Vs}	partial pressure of saturated vapour [Pa]	vs	Saturated vapor

References

[1] Iamsakulpanich, P., et al., Numerical simulation of porous media combustion for high temperature heat exchanger, *MATEC Web of Conferences*, 192 (2018)

[2] Alhusseny, A., et al., A POROUS MEDIA APPROACH FOR NUMERICAL OPTIMISATION OF THERMAL WHEEL, *Kufa Journal of Engineering*, 14 (2023), 4, pp. 56-68

[3] Lochan, R., zt al., Heat Transfer Improvement in Heat Exchanger using Porous Medium: a Review [Review of Heat Transfer Improvement in Heat Exchanger using Porous Medium: a Review], *International Journal of Innovative Research in Engineering & Management*, 3 (2016), 6, pp. 468-470

[4] Deptulski, R. C., et al., Flow and heat transfer in anisotropic active foam porous media wall, *MATEC Web of Conferences*, 330 (2020)

[5] Qader, F. F., et al., Enhancement of Double-Pipe Heat Exchanger Effectiveness by Using Porous Media and TiO2 Water. *CFD Letters*, 15 (2023), 4, pp. 31-42

[6] Carballo, A. A., et al., Numerical and experimental study of open-cell foams for the characterization of heat exchangers, *arXiv (Cornell University)*, 2023

[7] Carballo, A. A., et al., Numerical and experimental study of open-cell foams for the characterization of heat exchangers, *International Journal of Heat and Mass Transfer*, 217 (2023), 15

[8] Maes, J., Menke, H., GeoChemFoam: Direct modelling of flow and heat transfer in micro-CT images of porous media, *Heat and Mass Transfer*, 58 (2022), 11, pp. 1937-1947

[9] Deptulski, R. C., et al., Active wall through a porous media foam type: flow and transfer characterization, *MATEC Web of Conferences*, 330 (2020)

[10] Piller, M., et al., Pore-scale simulation of laminar flow through porous media, *Journal of Physics Conference Series*, 501 (2014)

[11] Zavattoni, S. A., et al., Conceptual design and performance evaluation of an innovative high temperature ceramic heat exchanger, *Journal of Physics Conference Series*, 2116 (2021), 1

[12] Das, S., et al., Direct numerical simulation for flow and heat transfer through random open-cell solid foams: Development of an IBM based CFD model, *Catalysis Today*, 273 (2016), pp. 140-150

[13] Skibiński, J., et al., Influence of Pore Size Variation on Thermal Conductivity of Open-Porous Foams, *Materials*, 12 (2019), 12

[14] Haussener, S., et al., *Tomography-Based Heat and Mass Transfer Characterization of Reticulate Porous Ceramics for High-Temperature Processing*, Heat Transfer summer conference, San Francisco, California, USA, 2009, pp. 33-44

[15] Pullar, R. C., et al., (2019). A Review of Solar Thermochemical CO2 Splitting Using Ceria-Based Ceramics With Designed Morphologies and Microstructures , *Frontiers in Chemistry*, 7 (2019)

[16] Kozhukhov, N. N., et al., Modeling of heat transfer in an element with anisotropic porosity, *Journal of Physics Conference Series*, 2039 (2021), 1

[17] Whitaker S., Simulation heat, mass and momentum transfer in porous media a theory of drying, *Advances in Heat Transfer*, 13 (1977), pp. 119-203

[18] Dittus F. W., Boelter L. M. K., Heat transfer in automobile radiators of the tubular type, *Int. Comm. Heat Mass Transfer*, 12 (1985), pp. 3–22.

[19] Incropera F. P., De Witt D. P., *Fundamentals, Heat and Mass Transfer*, John Wiley & Sons, New York, USA, 2002

[20] Rzig R., et al., Three-dimensional simulation of mass and heat transfer in drying unsaturated porous medium, *Heat Transfer Research*, 48 (2017), 11, pp. 985-1005

[21] Khedher N. B., Nasrallah S. B., Three-dimensional modeling and analysis of a porous thermal energy storage system, *Journal of Applied Fluid Mechanics*, 3 (2010)

Hussain A., et al., Heat and mass transfer in tubular ceramic membranes for membrane reactors, *International Journal of Heat and Mass Transfer*, 49 (2006), pp. 2239–2253